INTERIM REPORT

Accession No. ______________

____

Contract Program or Project Title: BWR Refill-Reflood Program

Subject of this Document: Program Progress

Type of Document: Monthly Letter

Author(s): G. W. Burnette

Date of Document: October 1979

Responsible NRC Individual and NRC Office or Division: W. D. Beckner

This document was prepared primarily for preliminary or internal use. It has not received full review and approval. Since there may be substantive changes, this document should not be considered final.

Prepared for
U.S. Nuclear Regulatory Commission
Washington, D.C. 20555

INTERIM REPORT

GENERAL ELECTRIC

NUCLEAR ENERGY

BUSINESS GROUP

GENERAL ELECTRIC COMPANY, 175 CURTNER AVE., SAN JOSE, CALIFORNIA 95125

November 12, 1979

Mr. Edward L. Halman, Director
Division of Contracts
U.S. Nuclear Regulatory Commission
Washington, D.C. 20555

Dr. M. Merilo
EPRI PMG Member, BWR-BD/EDD Program
Safety & Analysis Department
Electric Power Research Institute
P. O. Box 10412
Palo Alto, CA 94303

SUBJECT: BWR REFILL/REFLOOD PROGRAM
CONTRACT NO. NRC-04-79-184
INFORMAL MONTHLY PROGRESS REPORT FOR OCTOBER 1979

Gentlmen:

The following summarizes the subject matter covered in the attached report:

BWR/4 & 5 double nozzle testing has started in the 30° Sector Facility. Simulator nozzles have been developed and testing is underway. Shakedown testing of the Single Heated Bundle Facility has been completed. Detailed planning of the 30° Sector Facility modification has begun and development of the task plan document has started. TRAC compatible models for interfacial shear and CCFL are described.

Distribution of this report is being made in accordance with the "Monthly Distribution List" provided with W. D. Beckner's letter of September 6, 1979.

Very truly yours,

G W Burnette

G. W. Burnette, Manager
External Programs
M/C 583, Telephone (408) 925-5375

cc: RG Bock

GWB/td

1402 265

BWR REFILL-REFLOOD PROGRAM

THIRD MONTHLY REPORT

OCTOBER 1979

Prepared for:

Division of Reactor Safety Research
U.S. Nuclear Regulatory Commission
Washington, D.C. 20555
NRC FIN No. B5877

and

Electric Power Research Institute
3412 Hillview Avenue
Palo Alto, CA 94303
EPRI Project No. RP-1377-1

and

General Electric Company
175 Curtner Avenue
San Jose, CA 92125

By

General Electric Company

1402 266

Under

Contract No. NRC-04-79-184

REFILL-REFLOOD PROGRAM

THIRD MONTHLY REPORT

OCTOBER, 1979

SUMMARY

BWR/4 & 5 double nozzle testing has started in the 30° Sector Facility. Simulator nozzles have been developed and testing is underway. Shakedown testing of the Single Heated Bundle Facility has been completed. Detailed planning of the 30° Sector Facility modification has begun and development of the task plan document has started. TRAC comaptible models for interfacial shear and CCFL are described.

CORE SPRAY DISTRIBUTION (Task 4.2)

Tests were performed with the BWR/4 double nozzle assembly at the Lynn 30° Sector Steam Test Facility. Data packages are being prepared for transmittal to San Jose where they will be reviewed before initiating changeover for the Lower Sparger 30° Sector tests. Simulator nozzle tests at the Vallecitos Spray Facility have been completed and nozzle design information has been transmitted to Lynn for use in design of the 30° Sector air test hardware. An informal, interim data report covering the BWR/4 & 5 simulator nozzle development has been completed. Additional single nozzle tests at the Horizontal Spray Facility are being planned to begin in late November.

Reactor nozzle tests in steam are needed to extend the flow range and provide statistical data on repeatability. Additional simulator nozzle tests in air are also needed to improve the accuracy of the data at the low end of the flow range. Internal review of the Task Plan Report draft is continuing.

SINGLE HEATED BUNDLE TASK (Task 4.3)

Shakedown and calibration testing in the ECCS Test Loop was completed in preparation for Stage One testing. Stage One testing, which is characterized as system effects tests with a heated bundle, is scheduled to begin early in November. Data from the shakedown and calibration tests are being reviewed and evaluated. As reported last month, the Stage One Tests will be directed at: (1) confirming the scaling basis used to translate the TLTA transient test data to atmospheric conditions, and (2) providing a typical system response data base to be used in developing the adiabatic steam injection technique for the Lynn CCFL/Refill System Effects Tests in the 30° Sector facility. A draft of the Task Plan has been completed and is undergoing internal review.

CCFL/REFILL SYSTEM EFFECTS [30° Sector] (Task 4.4)

1) Task Plan

Work is continuing on development of the task plan. The activities necessary to complete the task plan have been identified and design information requirements have been formulated.

2) Facility Modification

The design support information required for completion of the test facility functional specifications and experiment measurement objectives has been specified in detail. The design support information includes: Blowdown system, isolation of excess steam volume, external loop requirements, measurement requirements, data reduction requirements, separate effects test requirements, and test initial conditions. Development of a completion schedule and detailed action plan is in progress.

Work continues on setting-up available analysis methods for the 30° sector facility simulation. Results from these studies, in conjunction with experimental data from the TLTA and SHB, will be used to evaluate scaling options, to perform sensitivity analyses, to determine test initial conditions, and ultimately to determine facility hardware requirements.

BASIC MODELS AND CORRELATIONS (Task 4.7.1)

Models for the interface shear and CCFL has been implemented into a developmental version of TRAC. A detailed writeup on this model is included as Appendix I.

The assessment of the constitutive correlations for shear and heat transfer in TRAC has continued in this period.

SINGLE CHANNEL CODE (Task 4.7.2)

The feasibility study for the single channel code has been continued. The study is based on a comparison of ATHENA (drift flux model) and the TRAC two fluid model. The main effort has been on the creation of input decks for a BDHT experiment to be used for the comparison and to make the necessary modifications to TRAC.

SUPPORT DEVELOPMENT OF TRAC BWR (Task 4.7.3)

The main emphasis has been on a further refinement of the component models and the BWR simulation. The jet pump-model has been developed to include all cases for positive drive flow. The BWR simulation has been modified to include the ECC systems and a more detailed modeling of the downcomer.

A meeting with INEL was held at GE on October 2, 1979; the purpose of the meeting was to coordinate the TRAC development efforts between GE and INEL. The activities needed for BD0/BD1 versions of TRAC were agreed upon, and responsibilities were established. The activities are given in Table I. It was furthermore agreed to divide the work between the two organizations as far as possible and to setup regular meetings to coordinate this work.

MODEL QUALIFICATION (4.8)

Work continues on data base classification and development of the Model Qualification Task Plan. The task plan document is about 50% complete.

GW Burnett
G. W. Burnette, Manager
External Programs

GWB/cat

TABLE I

ACTIVITIES AND RESPONSIBILITIES FOR TRAC BD0/BD1

NO.	ACTIVITY	PRIMARY RESPON.	VERSION BD0	VERSION BD1
1.	Model for leakage path (core to bypass)	EG&G	Use explicit source term	As in BD0 or zero-node tee
2.	Two Fluid One Dimensional Model (TF1D)	LASL	Use earlier version if final one not available	
3.	Axial conduction rewetting	EG&G/ GE	Outside of pipe	Incorporate from PD2 (to be assessed by GE)
4.	Assess numerical stability	EG&G	Assess	Implement improvements
5.	Upper plenum model	GE/ EG&G	Input source terms (EG&G)	Develop model for calculation of source distribution (GE)
6.	Initialization routine	EG&G	No	✓
7.	Entrainment calculations, Two-phase levels	GE	✓	Improve
8.	Assess Heat Transfer Correlations	GE	✓	---
9.	Code Structure changes	EG&G	✓	---
10.	ECC trip logic improvement	GE/ EG&G	No	✓
11.	Heat slab quench front model (for backup representation)	GE	✓	---

1402 270

Activities and Responsibilities for TRAC BD0/BD1 (Continued)

NO.	ACTIVITY	PRIMARY RESPON.	VERSION BD0	VERSION BD1
12.	Component models (jet pump, separators)	GE/ EG&G	Extend for TF1D (GE)	Improvements (GE, EG&G)
13.	CCFL/Interfacial Shear	GE/ EG&G	Extend to TF1D (GE)	Improve- (GE, EG&G)
14.	BWR input deck	EG&G/ GE	✓	---
15.	Radiation model	EG&G/ GE	Use current model (EG&G)	Refine to include anisotropic effects (GE)
16.	Water rod model	EG&G	Assess	✓
17.	Containment model	LASL	No	No
18.	Mass inbalance correction	LASL	If available (EG&G)	✓
19.	Momentum source model assessment	GE	✓	---

1402 271

APPENDIX I

Interfacial Shear in the BWR Version of TRAC

By

J. G. M. Andersen

R. F. Kimbrell

1402 272

TABLE OF CONTENTS

1402 273

1. INTRODUCTION

The constitutive correlations for the interface shear in TRAC[1] have beer assessed and modified in light of the two-phase flow phenomena in a BWR. It was found that the constitutive correlations for the interface shear in the two-fluid model and relative velocity in the drift flux model in TRAC did not predict the void fraction adequately, and furthermore that the two-fluid model and the drift-flux model gave inconsistent results.

New correlations have been developed for the relative velocity in the drift-flux model and for the interface shear in the two-fluid models. The correlations are based on available data[2] for the relative velocity and the void fraction, and on CCFL data.

The new correlations have been assessed, and it was found that: the drift-flux and the two-fluid models are consistent for steady state conditions; saturated CCFL and subcooled CCFL breakdown can be predicted; void fractions are predicted well for level swell tests.

2. WALL FRICTION AND INTERFACE SHEAR

The experimental data available for the evaluation of the wall friction and the interface shear for two-phase flow will generally be the pressure drop, the void fraction, and the flow rates for each phase.

For the drift-flux model the problem is to correlate the wall friction and the relative velocity between the phases. In TRAC[1], the drift-flux model is formulated as:

Mixture Continuity:

$$\frac{\partial \rho_m}{\partial t} + \frac{\partial}{\partial t}\left(\rho_m V_m\right) = 0 \tag{2.1}$$

Vapor Continuity:

$$\frac{\partial}{\partial t}\left(\alpha \rho_g\right) + \frac{\partial}{\partial t}\left(\alpha \rho_g V_m\right) + \frac{\partial}{\partial t}\left(\frac{\alpha(1-\alpha)\rho_l \rho_g}{\rho_m} V_r\right) = \Gamma \tag{2.2}$$

Mixture Momentum:

$$\frac{\partial}{\partial t} V_m + V_m \frac{\partial}{\partial t} V_m + \frac{1}{\rho_m}\frac{\partial}{\partial t}\left(\frac{\alpha(1-\alpha)\rho_l \rho_g}{\rho_m} V_r^2\right) = -\frac{1}{\rho_m}\frac{\partial P}{\partial z} - \frac{1}{\rho_m}\bar{F}_w + g \tag{2.3}$$

For steady-state conditions, and assuming Γ, α and the material properties are known, we have 3 equations and 3 unknowns:

V_m , V_r and F_w

and the problem can be directly solved.

The results are usually of the form:

$$F_w = F_w\,(V_m, \alpha\,,\ \text{geometry, material properties}) \tag{2.4}$$

$$V_r = V_r\,(V_m, \alpha,\ g,\ \text{geometry, material properties}) \tag{2.5}$$

For the two-fluid model the problem is to correlate the wall friction and the interface shear between the phases. The wall friction, however, must be distributed between the phases. In TRAC[1], the two-fluid model is formulated as:

Mixture Continuity:

$$\frac{\partial}{\partial t}\rho_m + \frac{\partial}{\partial z}\left((1-\alpha)\rho_l V_l + \alpha \rho_g V_g\right) = 0 \tag{2.6}$$

Vapor Continuity:

$$\frac{\partial}{\partial t}(\alpha \rho_g) + \frac{\partial}{\partial z}(\alpha \rho_g V_g) = \Gamma \tag{2.7}$$

Liquid Momentum:

$$\frac{\partial}{\partial t}V_l + V_l \frac{\partial}{\partial t}V_l = -\frac{1}{\rho_l}\frac{\partial P}{\partial t} + g + \frac{\Gamma}{(1-\alpha)\rho_l}(V_l - V_{il}) + f_{lg} - F_l \tag{2.8}$$

Vapor Momentum:

$$\frac{\partial}{\partial t}V_g + V_g \frac{\partial}{\partial z}V_g = -\frac{1}{\rho_g}\frac{\partial P}{\partial z} + g + \frac{\Gamma}{\alpha \rho_g}(V_{ig} - V_g) - f_{lg} - F_g \tag{2.9}$$

For steady state conditions, assuming that Γ, α, the interface velocities, and the material properties are known, we have 4 equations but 5 unknowns:

$$V_1,\ V_g,\ F_1,\ F_g,\ f_{lg}$$

and the problem cannot be directly solved. To obtain a solution information on how to partition the wall friction between the phases is necessary. The partitioning of the wall shear between the phases may be flow regime dependent, but once it is established, the interface shear can be correlated. The result is usually of the form:

$$f_{lg} = f_{lg}(V_1,\ V_g,\ \alpha\ ,\ \text{geometry, material properties}) \quad (2.10)$$

The relative velocity between the phases will, for steady state conditions, be given by the balance between the bouyancy and the shear, and consequently there must be a unique correspondence between the relative velocity, Equation (2.5) and the interface shear, Equation (2.10).

In the following paragraphs, a model for the partitioning of the wall friction between the phases will be developed, and the correspondence between the relative velocity and the interface shear will be demonstrated.

2.1 Partitioning of the Wall Friction Between the Phases

Following Ishii's notation[2] the local time averaged, momentum equations for the gas and liquid phases are

$$\alpha \rho_g \left(\frac{\partial \bar{v}_g}{\partial t} + \bar{v}_g \cdot \nabla \bar{v}_g \right) = -\alpha \nabla P + \alpha \nabla \cdot \bar{\bar{\tau}} - \alpha \rho_g \bar{g} - \bar{M}_g \tag{2.11}$$

$$(1-\alpha) \rho_l \left(\frac{\partial \bar{v}_l}{\partial t} + \bar{v}_l \cdot \nabla \bar{v}_l \right) = -(1-\alpha) \nabla P + (1-\alpha) \nabla \cdot \bar{\bar{\tau}} - (1-\alpha) \rho_l \bar{g} - \bar{M}_l \tag{2.12}$$

Here the interfacial mass transfer has been neglected, and M must obey

$$M_g + M_l = 0 \tag{2.13}$$

For one-dimensional flow Equations (1) and (2) degenerate to

$$\alpha \rho_g \left(\frac{\partial v_g}{\partial t} + v_g \frac{\partial v_g}{\partial z} \right) = -\alpha \frac{\partial P}{\partial z} + \alpha \nabla \cdot \bar{\bar{\tau}}_z - \alpha \rho_g g - M_g \tag{2.14}$$

$$(1-\alpha) \rho_l \left(\frac{\partial v_l}{\partial t} + v_l \frac{\partial v_l}{\partial z} \right) = -(1-\alpha) \frac{\partial P}{\partial z} + (1-\alpha) \nabla \cdot \bar{\bar{\tau}}_z - (1-\alpha) \rho_l g - M_l \tag{2.15}$$

An interpretation of the various terms on the right hand side of Equations (2.14) and (2.15) can be obtained from Figure 1:

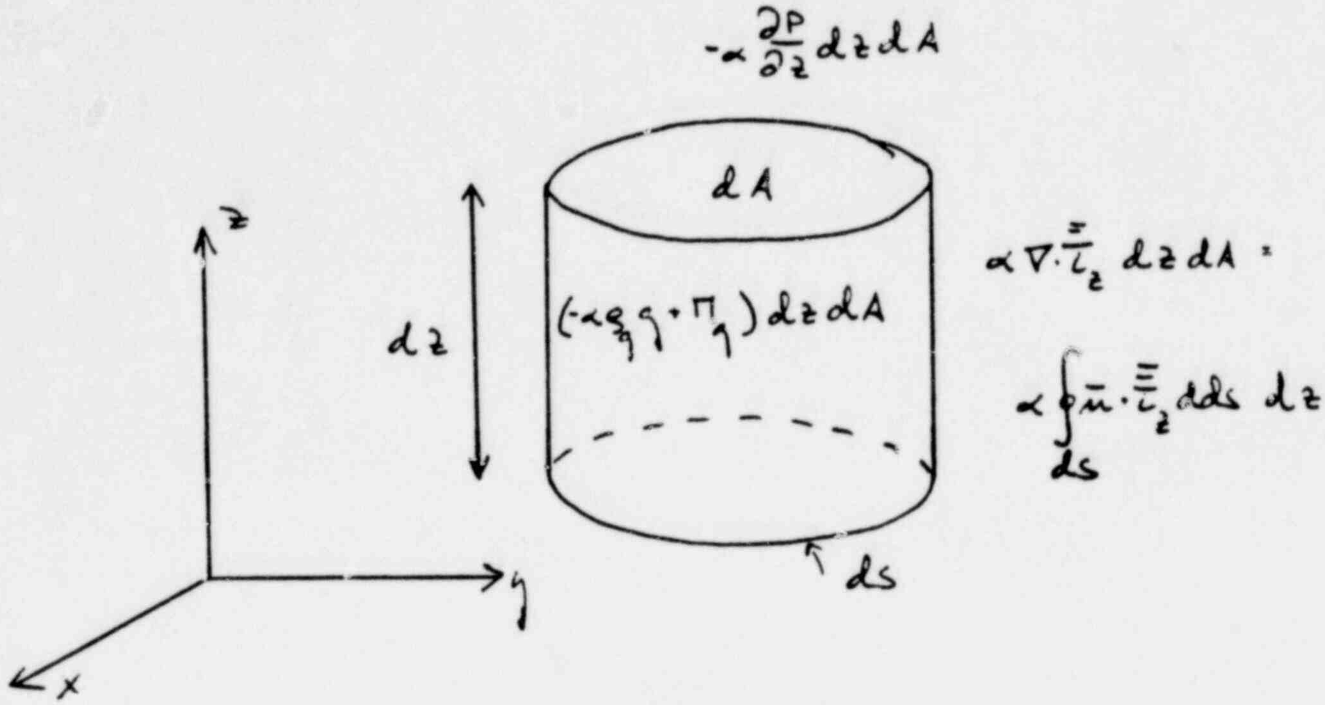

FIGURE 1. R.h.s. of Vapor Momentum Equation

For the gas equation the interpretation of the various terms are:

$-\alpha \frac{\partial P}{\partial z}$ is the force on the gas due to the pressure gradient in the Z direction, **the pressure is assumed** to be constant for constant Z, and the same for each phase.

$\alpha \nabla \cdot \bar{\bar{\tau}}_z$ is the force on the gas due to the shear at the surface of the incremental volume, α is the fraction of the surface which is occupied by the gas. It is assumed that $\frac{\partial}{\partial z} \bar{\bar{\tau}}_z = 0$. It is furthermore assumed that the averaged shear tensor is the same for each phase, which is reasonable, since except for surface tension effects the shear is a continuous function.

$-\alpha \rho_g g$ is the body force, due to gravity, on the gas.

M_g is the interfacial drag between the phases inside the incremental volume due to local difference in the phase velocities.

In order to partition the wall friction and derive the interfacial drag coefficients, steady state, adiabatic flow is considered, consistent with the assumption that these quantities are not affected by transient conditions.

$$\alpha \frac{\partial P}{\partial z} - \alpha \nabla \cdot \bar{\bar{\tau}}_z + \alpha \rho_g g + \Pi_g = 0 \tag{2.16}$$

$$(1-\alpha) \frac{\partial P}{\partial z} - (1-\alpha) \nabla \cdot \bar{\bar{\tau}}_z + (1-\alpha) \rho_\ell g - \Pi_g = 0 \tag{2.17}$$

Adding Equations (2.16) and (2.17) we obtain:

$$\frac{\partial P}{\partial z} - \nabla \cdot \bar{\bar{\tau}}_z + ((1-\alpha)\rho_\ell + \alpha \rho_g) g = 0 \tag{2.18}$$

Integrating this equation over the cross section, and assuming that ρ_ℓ and ρ_g are only functions of z we get:

$$A \frac{\partial P}{\partial z} - \oint \bar{n} \cdot \bar{\bar{\tau}}_{wz} \, dS + A(\langle 1-\alpha \rangle \rho_\ell + \langle \alpha \rangle \rho_g) g = 0 \tag{2.19}$$

Where the integral is along the boundary (w), n is the normal to the boundary, and Gauss's theorem has been used. Combining (2.18) and (2.19) we obtain:

$$\nabla\cdot\bar{\bar{\tau}}_z = \frac{1}{A}\oint \bar{n}\cdot\bar{\bar{\tau}}_{wz}\,ds - \Delta\rho g(\alpha - \langle\alpha\rangle) \tag{2.20}$$

Integrating the momentum equation for the gas over the cross section we get:

$$\langle\alpha\rangle A\frac{\partial P}{\partial z} - \int_A \alpha\nabla\cdot\bar{\bar{\tau}}_z\,dA + \langle\alpha\rangle\rho_g g + \int_A \Pi_g\,dA = 0 \tag{2.21}$$

The second term in this equation can be evaluated using (2.20):

$$\begin{aligned}\int_A \alpha\nabla\cdot\bar{\bar{\tau}}_z\,dA &= \int_A\left(\frac{\alpha}{A}\oint \bar{n}\cdot\bar{\bar{\tau}}_{wz}\,ds - \Delta\rho g\alpha(\alpha-\langle\alpha\rangle)\right)dA \\ &= \langle\alpha\rangle\oint \bar{n}\cdot\bar{\bar{\tau}}_{wz}\,ds - A\Delta\rho g\langle(\alpha-\langle\alpha\rangle)^2\rangle\end{aligned} \tag{2.22}$$

Now, the first term on the right hand side of (2.20) is nothing but the wall shear, $-F_w$. Consequently, we have:

$$\int_A \alpha\nabla\cdot\bar{\bar{\tau}}_z\,dA = -\langle\alpha\rangle F_w - A\Delta\rho g\langle(\alpha-\langle\alpha\rangle)^2\rangle \tag{2.23}$$

Inserting this in Equation (2.21) we get

$$\begin{aligned}\langle\alpha\rangle A\frac{\partial P}{\partial z} + \langle\alpha\rangle F_w + \langle\alpha\rangle A\rho_g g + \int_A \Pi_g\,dA \\ + A\Delta\rho g\langle(\alpha-\langle\alpha\rangle)^2\rangle = 0\end{aligned} \tag{2.24}$$

Similarly for the liquid momentum equation we get

$$\langle 1-\alpha\rangle A \frac{\partial P}{\partial z} + \langle 1-\alpha\rangle F_w + \langle 1-\alpha\rangle \rho_l g A - \int_A \Pi_g \, dA - A \Delta\rho g \langle(\alpha - \langle\alpha\rangle)^2\rangle = 0 \qquad (2.25)$$

The physical interpretation of the various terms in the integrated momentum equation for the gas are:

$\langle\alpha\rangle A \frac{\partial P}{\partial z}$ The force due to the pressure gradient.

$\langle\alpha\rangle F_w$ **The force on the vapor due to the shear field** created by the wall-friction.

$\langle\alpha\rangle A \rho_g g$ The body force due to gravity.

$\int_A \Pi_g \, dA$ The drag force between the phases due to local velocity differences.

$A\Delta\rho g \langle(\alpha - \langle\alpha\rangle)^2\rangle$ Interfacial shear (see Equation 2.20) created by the uneven void distribution.

The terms in the integrated liquid momentum equation can, of course, be interpreted in the same way.

Consequently, if the liquid phase alone is in contact with the wall, the wall-friction acts alone on the liquid and we have:

$F_g = 0$

$F_l = F_w$

The shear field, however, caused by the wall friction, creates an interfacial shear between the phases given by

$$\langle\alpha\rangle F_w$$

and the total forces on the phases due to the wall friction become:

1402 282

$\langle\alpha\rangle F_w$ for the gas phase

$\langle 1-\alpha\rangle F_w$ for the liquid phase

Similarly, if the gas-phase is in contact with the wall, we have

$$F_g = F_w$$

$$F_1 = 0$$

and the interfacial shear, due to the wall friction, becomes:

$$\langle 1-\alpha\rangle F_w$$

With the paritioning of the wall shear as given by Equation (2.14) and (2.15), the number of unknowns in Equations (2.6) - (2.9) is reduced to 4: V_1, V_g, F_w, and f_{ig}, and the interface shear can be calculated*.

2.2 Interface Drag and Phase Distribution

Eliminating $\frac{\partial p}{\partial z}$ and $\bar{\bar{\tau}}_z$ from Equation (2.16) and (2.17) gives:

$$\Pi_g = \alpha(1-\alpha)\Delta\rho g \tag{2.26}$$

---

* It is interesting to note that any partitioning of the wall shear fulfilling $F_1 + F_g = F_w$ is mathematically possible when the space averaged equations are used. The above partitioning, however, leads to the simple correlation of the interfacial drag. It is indeed the only partitioning that leaves the drag independent of the wall friction.

Locally, the drag is equal to the bouyancy. Integrating this equation over the cross section gives

$$\int \Pi_g \, dA = A \Delta\rho g \langle \alpha(1-\alpha) \rangle \qquad (2.27)$$

If $\int \Pi_g \, dA$ can be obtained from void fraction and pressure drop data we can correlate:

$$\eta = \frac{\langle \alpha(1-\alpha) \rangle}{\langle \alpha \rangle \langle 1-\alpha \rangle} \qquad (2.28)$$

$$= \frac{\int \Pi_g \, dA}{A \Delta\rho g \langle \alpha \rangle \langle 1-\alpha \rangle} \qquad (2.29)$$

Consequently, the magnitude of the interface drag yields information on the void distribution.

For fully dispersed flow, $\alpha \approx \langle \alpha \rangle$, and we get $\eta \approx 1$ or

$$\int \Pi_g \, dA \approx A \Delta\rho g \langle \alpha \rangle \langle 1-\alpha \rangle$$

On the other hand, for fully separated flow, $\alpha(1-\alpha)$ = 0, and we get η = 0 or

$$\int \Pi_g \, dA \approx 0$$

In the case of fully separated flow there is no local drag between the phases, but there is a shear at the interface. For ideal annular flow the shear from Figure 2.24 will be

$$-\langle \alpha \rangle F_w - \langle \alpha \rangle \langle 1-\alpha \rangle A \Delta\rho g$$

where the first term is due to the wall shear and the second one due to the non-uniform void distribution.

Locally, the interface drag must be related to the velocity difference of the phases; let us define:

$$M_g = C_i \, |V_g - V_\ell| (V_g - V_\ell) \tag{2.30}$$
$$= C_i \, |V_R| \, V_R$$

C_i in the above expression has a dimension, and it would be more logical to define the interface drag in terms of a drag coefficient

$$M_g = \frac{1}{8} \frac{C_D}{d_i} \rho^* |V_R| V_R$$

where ρ^* is a suitable density and d_i is the interface area per unit volume. However, without additional assumptions only $C_i = \frac{1}{8} \frac{C_D}{d_i} \rho^*$ can be directly correlated from data. In the present work only the correlation of C_i will be assessed. Integrating (2.30) over the cross section we get,

$$\int M_g \, dA = A \bar{C}_i \, |\bar{V}_R| \, \bar{V}_R \tag{2.31}$$

where

$$\bar{V}_R = \frac{\langle f(\alpha) V_R \rangle}{\langle f(\alpha) \rangle} \tag{2.32}$$

$$\bar{C}_i = \frac{\langle C_i |V_R| V_R \rangle \langle f(\alpha) \rangle^2}{|\langle f(\alpha) V_R \rangle| \langle f(\alpha) V_R \rangle} \tag{2.33}$$

and f(α) is a weighting function. For dispersed flow, the concentration of the dispersed phase would be a logical choice. A function that meets this criteria for both $\alpha \to 0$ and $\alpha \to 1$ is

$$f(\alpha) = \alpha(1-\alpha) \tag{2.34}$$

It is important to note that

$$\bar{V}_r \neq \bar{V}_g - \bar{V}_l \tag{2.35}$$

where
$$\bar{V}_g = \frac{\langle \alpha V_g \rangle}{\langle \alpha \rangle}$$

$$\bar{V}_l = \frac{\langle (1-\alpha) V_l \rangle}{\langle 1-\alpha \rangle}$$

$\bar{V}_g$ and $\bar{V}_l$ have different weight functions.[4] Using that

$$V_r = \frac{V_{gj}}{1-\alpha} ,$$

inserting it in (2.32) and using (2.28) we get,

$$\bar{V}_r = \frac{1}{\eta} \frac{\bar{V}_{gj}}{\langle 1-\alpha \rangle} . \tag{2.36}$$

where
$$\bar{V}_{gj} = \frac{\langle \alpha V_{gj} \rangle}{\langle \alpha \rangle}$$

Combining (2.31) and (2.36), we get,

$$\int M_g \, dA = A \bar{C}_i \frac{|\bar{V}_{gj}| \bar{V}_{gj}}{\langle 1-\alpha \rangle^2 \eta^2} \tag{2.37}$$

If $\bar{V}_{gj}$ can be correlated from void-fraction data, $\bar{C}_i$ can be correlated.

Combining (2.27) with (2.37) gives

$$\bar{C}_i \frac{|\bar{V}_{gj}| \bar{V}_{gj}}{\langle 1-\alpha \rangle^2 \eta^2} = \Delta\rho g \langle \alpha \rangle \langle 1-\alpha \rangle \eta \tag{2.38}$$

or

$$\bar{C}_i = \frac{\Delta\rho g \langle \alpha \rangle \langle 1-\alpha \rangle^3}{|\bar{V}_{gj}| \bar{V}_{gj}} \eta^2 \tag{2.39}$$

With η and $\bar{V}_{gj}$ correlated from void fraction and pressure drop data, the interface drag coefficient $\bar{C}_i$ can be determined.

Using the identity:

$$\bar{V}_g = C_0 \langle j \rangle + \bar{V}_{gj} \tag{2.40}$$

where

$$C_0 = \frac{\langle \alpha j \rangle}{\langle \alpha \rangle \langle j \rangle} \tag{2.41}$$

and combining with (2.36) we get

$$\bar{V}_R = \frac{1}{\eta}\left[\frac{1-\langle\alpha\rangle C_o}{\langle 1-\alpha\rangle}\bar{V}_g - C_o\bar{V}_\ell\right] \tag{2.42}$$

If C_o can be correlated from void fraction data $\bar{V}_R$ can be calculated. Combining (2.37) and (2.42) gives

$$\int M_g dA = \bar{C}_i \frac{1}{\eta^2}\left|\frac{1-\langle\alpha\rangle C_o}{\langle 1-\alpha\rangle}\bar{V}_g - C_o\bar{V}_\ell\right|\left(\frac{1-\langle\alpha\rangle C_o}{\langle 1-\alpha\rangle}\bar{V}_g - C_o\bar{V}_\ell\right) \tag{2.43}$$

With $\bar{C}_i$, η and C_o correlated from void fraction and pressure drop data, the interface drag can be calculated.

Note that for horizontal flow, there is no local drag and In this case $\bar{C}_i$ is indeterminant from Equation (3.29). However, Equation (2.43) will predict unequal average velocities due to the uneven velocity and void profiles (C_o effect).

2.3 Discussion

The main assumptions in the model for the wall friction and the interface shear are:

- The interface drag coefficient derived for steady state conditions is applicable for transient conditions.
- The phase and velocity distributions found for steady state conditions are applicable for transient conditions.

1402 288

The main conclusions of the model are:

- The shear on the phases due to the wall friction should be partitioned proportional to the concentration of the phases.
- The interface drag should be based on the average of the velocity difference rather than the difference between the average velocities.
- The formulation allows calculation of the interface drag in terms of "drift flux" parameters $\bar{V}_{gj}$, C_o which have a large data base for steady state conditions.

3. INTERFACIAL SHEAR AND CCFL

The three dimensional vessel component in TRAC[1] uses a six-equation two-fluid model. This model requires a formulation for interfacial shear which should be consistent with the drift flux model in the one-dimensional components. An additional requirement for this formulation is to predict the counter current flow limitation (CCFL). Unfortunately, there is a lack of data for void fraction and relative velocities under CCFL conditions, and existing models do not give good predictions. This section deals with the modifications to drift flux parameters due to Ishii[2] to predict CCFL, and use of the model to determine the interfacial shear terms.

The drift flux parameters that will be forced to the CCFL phenomena are described below:

$$C_o = a - \frac{b}{\gamma} = C_o' \qquad 0 \le \alpha < \alpha_1 \tag{3.1}$$

$$C_o = 1 + (C_o' - 1)\,\frac{1-\alpha}{1-\alpha_1} \qquad \alpha_1 \le \alpha \le 1 \tag{3.2}$$

$$\bar{V}_{gj} = k\,V_o \tag{3.3}$$

$$\bar{V}_{gj} = k \gamma V_o (1-\alpha) \quad \text{as } \alpha \text{ approaches 1.0} \tag{3.4}$$

$$\gamma = \sqrt{\frac{\rho_l}{\rho_g}} \tag{3.5}$$

$$V_o = \left(\frac{\Delta\rho\, g\, \sigma}{\rho_l^2}\right)^{0.25} \tag{3.6}$$

1402 290

This model must be modified to predict the CCFL phenomena, which is predicted by

$$\sqrt{j_g/j_{go}} + m\sqrt{j_l/j_{lo}} = 1 \tag{3.7}$$

$$j_{lo} = -cV_o \tag{3.8}$$

$$j_{go} = \gamma c V_o = -\gamma j_{lo} \tag{3.9}$$

The vapor volumetric flux can be determined from Equation (3.7)

$$j_g = j_{go}\left(1 - m\sqrt{j_l/j_{lo}}\right)^2 \tag{3.10}$$

Similarly, it can be determined from the drift flux model

$$j_g = \frac{\alpha C_o}{1-\alpha C_o} j_l + \frac{\alpha}{1-\alpha C_o}\bar{V}_{gj} \tag{3.11}$$

Eliminating j_g from the two equations allows the determination of the interception point between the two models. Defining

$$\bar{V}_{gj} = -F j_{lo} \tag{3.12}$$

$$x = \sqrt{-j_\ell} \tag{3.13}$$

we obtain

$$\left(m^2\gamma + \frac{\alpha C_o}{1-\alpha C_o}\right)x^2 - \left(2m\gamma\sqrt{-j_{\ell o}}\right)x - j_{\ell o}\left(\gamma - \frac{\alpha F}{1-\alpha C_o}\right) = 0 \tag{3.14}$$

For the drift flux model to be tangent to the CCFL correlation, the solution of Equation (3.14) must have a double root. Therefore, after simplification, we have

$$(1-\alpha C_o)(C_o - m^2F)\gamma - \alpha C_o F = 0 \tag{3.15}$$

Solving for the void fraction, we obtain the interception between the two models

$$\alpha_c = \frac{(C_o - m^2F)\gamma}{C_o\left((C_o - m^2F)\gamma + F\right)} \tag{3.16}$$

For $\alpha < \alpha_c$ Equation (3.14) has no solutions, and for $\alpha > \alpha_c$ there are two solutions. Consequently for $\alpha > \alpha_c$ the unmodified drift flux model would allow liquid downflow exceeding the CCFL correlation.

The modification to the drift flux parameters will be based on the assumptions (see Figure 2):

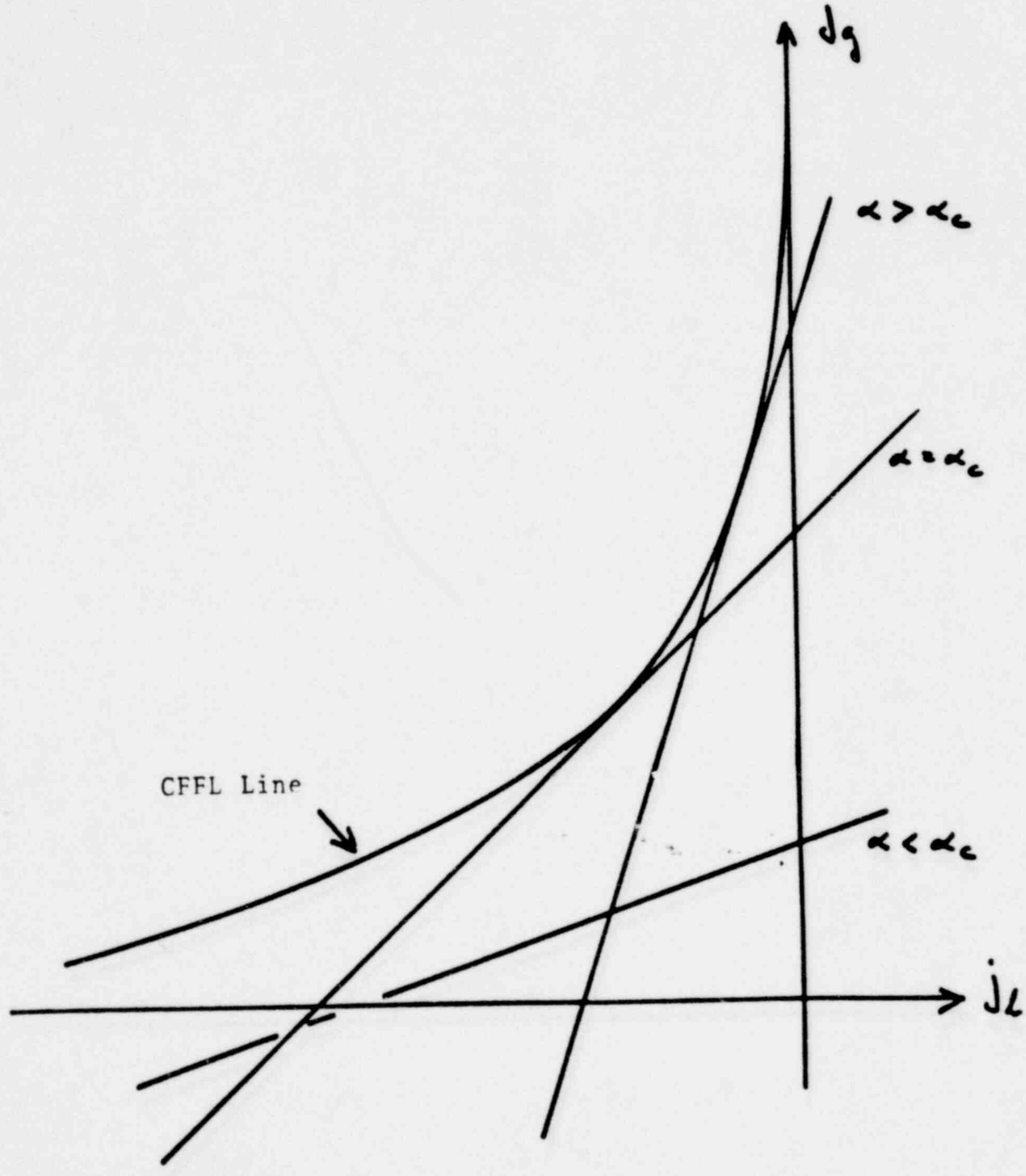

FIGURE 2 CCFL Model

1402 293

- For $\alpha < \alpha_c$ we have bubbly, slug, or churn.
- For $\alpha \geq \alpha_c$ we have dispersed annular flow, and CCFL will occur in this regime.

Consequently, C_o and F must be modified in such a way that the drift flux model is tangent to the CCFL correlation. Solving Equation (3.15) for C_o we obtain:

$$C_o = y + \sqrt{y - m^2 \frac{F}{\alpha}} \tag{3.17}$$

where

$$y = \frac{1}{2}\left(\frac{1}{\alpha} + F\left(m^2 - \frac{1}{\gamma}\right)\right) \tag{3.18}$$

which gives C_o as a function of F and void fraction. From Equations (3.2), (3.8), and (3.12), we see that F must approach $\frac{k\gamma}{c}(1-\alpha)$ as the void fraction approaches 1.0 and must be equal to K/C when the void fraction equals α_c. Assuming a function of the form

$$F = \frac{k}{c}\gamma(1-\alpha)\frac{1}{u} \tag{3.19}$$

$$u = \frac{1-\alpha}{1-\alpha_c}\left((1-\alpha_c)\gamma - \alpha_c\right) + \alpha \tag{3.20}$$

satisfies these two requirements The above drift flux model (specified in Equations (3.1) through (3.6), (3.12), and (3.16) through (3.20)) is in agreement with Ishii for bubbly, churn, and droplet flow and is modified to match the CCFL correlation for transition and annular flow. In Figure 3 C_o and $\bar{V}_{gj}$ are shown as a function of α.

We can use the above model in the one dimensional components, but we need an equivalent specification for the interfacial shear coefficients for the three dimensional vessel. The interfacial shear (f_{1g}) in TRAC is represented by a constant times the relative velocity squared. In Section 2, it is shown that the most appropriate form for vertical flow would be

$$f_{lg} = \bar{C}_i |\bar{V}_R| \bar{V}_R = \alpha(1-\alpha)\Delta\rho g \eta \tag{3.21}$$

where

$$\bar{V}_R = \frac{1}{\eta}\left(\frac{1-\alpha C_o}{1-\alpha}\bar{V}_g - C_o \bar{V}_l\right) = \frac{\bar{V}_{gj}}{\eta(1-\alpha)} \tag{3.22}$$

In the present model, we assume that η equals 1.0 to obtain the coefficient for interfacial shear.

$$\bar{C}_i = \frac{\alpha(1-\alpha)^3 \Delta\rho g}{\bar{V}_{gj}^2} \tag{3.23}$$

1402 295

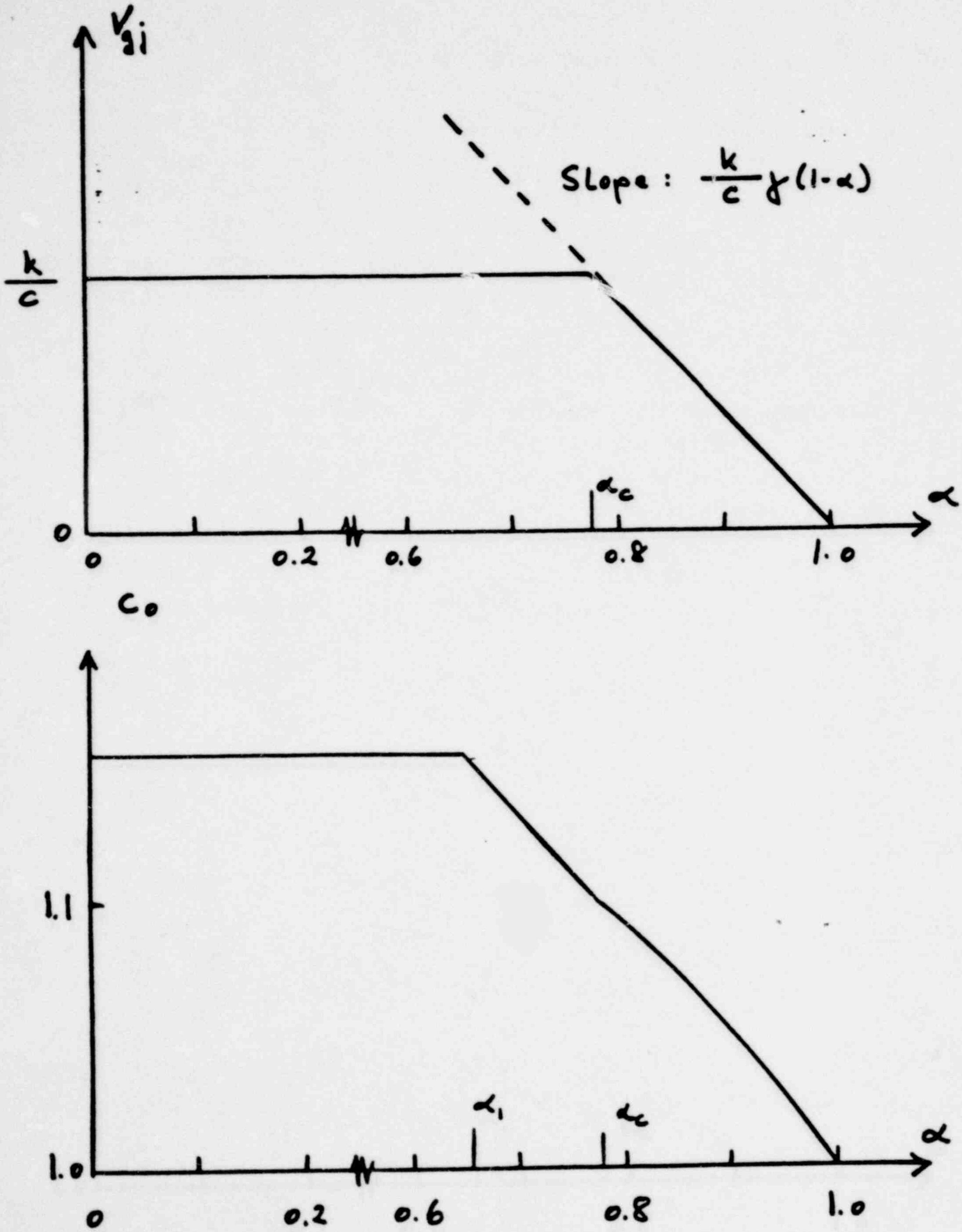

FIGURE 3 V_{gj} and C_o for P=70 Bar

1102 296

$\overline{V}_{gj}$ is determined from the above drift flux model. This coefficient is also used for horizontal flow. For horizontal flow, where no driving force (buoyancy) exists, the average of the relative velocity will be zero at steady state conditions. For 3-D flows, $\overline{V}_R$ in Equation (3.21) has to be treated as a vector; therefore, the axial component of the interfacial shear becomes $\overline{c}_i \, |\overline{V}_R| \, \overline{V}_{Rz}$. The model will be extended in the future with a correlation of η . The interfacial shear and drift flux models are now consistent and approach the CCFL conditions.

The actual CCFL correlation must still be imposed on the solution of the three dimensional momentum equations. The conservation equations in TRAC convect two different void fractions across the restriction, which could allow more liquid downflow than the correlation predicts. Using a relationship of the Kutaladze numbers (a different form of the CCFL equation used above), the counter current flow limiation is described by:

$$\sqrt{K_g} + m\sqrt{-K_\ell} = \sqrt{K} \tag{3.24}$$

where

$$K_g = \frac{\alpha \overline{V}_g \sqrt{\rho_g}}{(\Delta \rho g \sigma)^{0.25}} \tag{3.25}$$

$$K_\ell = \frac{(1-\alpha)\overline{V}_\ell \sqrt{\rho_\ell}}{(\Delta \rho g \sigma)^{0.25}} \tag{3.26}$$

The solution of the Z momentum equation is checked to determine if the vapor velocity is less than the relative velocity and if the vapor velocity is positive. If both conditions hold, the liquid velocity is compared to the liquid velocity obtained from the above equation, i.e.:

$$V_l' = \frac{-(g\sigma\Delta\rho)^{1/4}}{(1-\alpha)\sqrt{\rho_l}}\left(\sqrt{K} - \sqrt{K_g}\right)^2 \qquad (3.27)$$

If the negative liquid velocity is less than $\bar{V}_l'$, the liquid velocity is set to $\bar{V}_l'$: otherwise, no action is taken. Since the equations are linearized and a derivative term exists to correct for pressure drop changes, the derivative terms for the liquid velocity must also be changed if the liquid velocity is forced to the limit. The derivative term for the liquid velocity in this case becomes:

$$\frac{\partial V_l}{\partial \Delta P} = \left(\sqrt{\frac{K(g\sigma\Delta\rho)^{1/4}\,\alpha\sqrt{\rho_g}}{(1-\alpha)^2\rho_l V_g}} - \frac{\alpha\sqrt{\rho_v}}{(1-\alpha)\sqrt{\rho_l}}\right)\frac{\partial V_g}{\partial \Delta P} \qquad (3.28)$$

This equation is found by differentiating Equation (3.27) by the pressure drop with the vapor velocity assumed to be a function of the pressure drop.

With the inclusion of the above equations, TRAC calculates the counter current flow limit as defined by Equation (3.24).

To dampen velocity oscillations calculated by the vessel component in TRAC it was found necessary to add virtual mass terms also to the momentum equations. These oscillations were found while attempting to execute a simple CCFL model in TRAC. While the pressure and void fraction would essentially reach steady state relatively early, the velocities would continue to oscillate rather severely ($\sim$10 m/sec about a velocity of 14 m/sec). These oscillations caused the time for convergence to be extended and the number of time steps to reach steady state to be artifically large .

The virtual mass terms were included in the momentum equations by modifying the equations as follows:

$$\frac{D\bar{V}_g}{Dt} + \frac{\rho_c}{\rho_g}\left(\frac{\partial \bar{V}_g}{\partial t} - \frac{\partial \bar{V}_l}{\partial t}\right) = RHS^{*} \tag{3.29}$$

where:

ρ_c is the density of the continuous phase = $\left((1-\alpha)\sqrt{\rho_l} + \alpha\sqrt{\rho_g}\right)^2$

The liquid equation is treated similarly with the sign for ρ_c changed. The terms in the above form can be included in the implicit form of the momentum equations.

From the CCFL correlation the following* expression for the relative velocity can be derived

$$\bar{V}_g - \bar{V}_1 = \frac{K\,(\Delta\rho g \sigma)^{1/4}}{(1-\alpha)\sqrt{\rho_l} + \alpha\sqrt{\rho_g}} \tag{3.30}$$

1402 299

* Right han' side of momentum equation.

Comparing this expression to standard correlations for the relative velocity for various flow regimes, the term $((1-\alpha)\sqrt{\rho_\ell} + \alpha\sqrt{\rho_g})^2$ may be interpreted as the density of the continuous phase. Only the time derivative of the virtual mass is included in the momentum equation. This term is the most important for the damping of oscillations, and with the present state of the art the correct formulation of the spatial derivative is not known.

These terms may not be nesessary in the future because J. H. Mahaffy[5] has devised a method for enhancing stability in two phase flow calculations. If it is determined that they are not necessary upon implementation of the new 2F-1D model, they will be removed.

4. IMPLEMENTATION INTO TRAC

The implementation of the above drift flux and interfacial shear models into TRAC was conducted in a straight forward manner by modifying the subroutines TF3DE, FDMX3E, and SLIP. Additional modifications will be made when the two fluid one dimensional model is completed by LASL. These modifications will consist of constructing a subroutine to calculate the interfacial shear coefficient ($\bar{C}_i$) and inserting subroutine calls wherever the coefficient is required.

The drift flux model is used in SLIP to calculate the relative velocity. Using the definition for $\bar{V}_R$, (from Equation (3.22)), we have the following

$$(1-\alpha C_o)\bar{V}_g - (1-\alpha)C_o\bar{V}_l = \bar{V}_{gj} \qquad (4.1)$$

Since the mixture velocity is known and is determined by

$$\frac{(1-\alpha)\rho_l}{\rho_m}\bar{V}_l + \frac{\alpha\rho_g}{\rho_m}\bar{V}_g = V_m \qquad (4.2)$$

where

$$\rho_m = (1-\alpha)\rho_l + \alpha\rho_g \qquad (4.3)$$

we have two equations to determine $\bar{V}_g$ and $\bar{V}_l$. Solving these equations we have

$$V_{R,TRAC} = \bar{V}_g - \bar{V}_l = \frac{(\bar{V}_{gj} + (C_o-1)V_m)}{h\,(1-\alpha)} \qquad (4.4)$$

POOR ORIGINAL

where

$$h = \frac{((1-\alpha C_0)\rho_\ell + \alpha C_0 \rho_g)}{\rho_m} \tag{4.5}$$

This will make the relative velocity determined by the drift flux model consistent with the vapor and liquid velocities calculated by the interfacial shear model.

The two fluid model is used in FDMX3E and TF3DE, where the momentum equation is solved. With the new models for the interface shear and the virtual mass, the momentum equations in TRAC, e.g., for the axial direction, becomes

$$V_{\ell z_i}^{n+1} - V_{\ell z_i}^{n} + \frac{\Delta t}{\Delta x} V_{\ell z_i}^{n}\left(V_{\ell z_i}^{n} - V_{\ell z_{i-1}}^{n}\right) - \frac{\hat{\varsigma}_i}{\rho_{\ell_i}^{n}}\left(V_{gz_i}^{n+1} - V_{gz_i}^{n} - V_{\ell z_i}^{n+1} + V_{\ell z_i}^{n}\right) =$$

$$- \frac{\Delta t}{\Delta x_i}\frac{1}{\rho_{\ell_i}^{n}}\left(P_i^{n+1} - P_{i-1}^{n+1}\right) + \frac{\Delta t\,\Gamma_i^{n}}{(1-\alpha_i^{n})\rho_{\ell_i}^{n}}\left(V_{\ell z_i}^{n} - V_{i\ell z_i}^{n}\right) + g_z \Delta t \tag{4.6}$$

$$- \Delta t\,\hat{C}_{\ell z_i}\left|V_{\ell_i}^{n}\right| V_{\ell z_i}^{n+1} + \bar{C}_i^{n}\left|\frac{1-\alpha_i^{n} C_{0_i}^{n}}{1-\alpha_i^{n}} V_{g_i}^{n} - C_{0_i}^{n} V_{\ell_i}^{n}\right|\left(\frac{1-\alpha_i^{n} C_{0_i}}{1-\alpha_i^{n}} V_{gz_i}^{n+1} - C_{0_i}^{n} V_{\ell z_i}^{n+1}\right)\Delta t$$

and

$$V_{gz_i}^{n+1} - V_{gz_i}^{n} + \frac{\Delta t}{\Delta x} V_{gz_i}^{n}\left(V_{gz_i}^{n} - V_{gz_{i-1}}^{n}\right) + \frac{\hat{\varsigma}_i}{\rho_{g_i}^{n}}\left(V_{gz_i}^{n+1} - V_{gz_i}^{n} - V_{\ell z_i}^{n+1} + V_{\ell z_i}^{n}\right) =$$

$$- \frac{\Delta t}{\Delta x_i}\frac{1}{\rho_{g_i}^{n}}\left(P_i^{n+1} - P_{i-1}^{n+1}\right) - \frac{\Delta t\,\Gamma_i^{n}}{\alpha_i^{n}\rho_{g_i}^{n}}\left(V_{gz_i}^{n+1} - V_{igz_i}^{n+1}\right) + g_z \Delta t \tag{4.7}$$

$$- \Delta t\,\hat{C}_{gz_i}\left|V_{g_i}^{n}\right| V_{gz_i}^{n+1} - \Delta t\,\bar{C}_i^{n}\left|\frac{1-\alpha_i^{n} C_{0_i}^{n}}{1-\alpha_i^{n}} V_{g_i}^{n} - C_{0_i}^{n} V_{\ell_i}^{n}\right|\left(\frac{1-\alpha_i^{n} C_{0_i}^{n}}{1-\alpha_i^{n}} V_{gz_i}^{n+1} - C_{0_i}^{n} V_{\ell z_i}^{n+1}\right)$$

1402 302

where it has been assumed that V_{gz} and V_{lz} are positive in the donor cell differencing, V_g and V_l are the velocities on vector form, and V_{gz} and V_{lz} are the axial component of the velocities. Equations (4.6) and (4.7) constitute a system of linear equations in $V_{gz,i}^{n+1}$ and $V_{lz,i}^{n+1}$, and the solution will be of the form

$$V_{lz,i}^{n+1} = V_{lz,i}^{explicit} + K_{lz,i}\left(P_i^{n+1} - P_{i-1}^{n+1}\right) \tag{4.8}$$

$$V_{gz,i}^{n+1} = V_{gz,i}^{explicit} + K_{gz,i}\left(P_i^{n+1} - P_{i-1}^{n+1}\right) \tag{4.9}$$

which is consistent with the numerical method in TRAC. For the radial and theta-direction the momentum equations are solved in a similar way.

5. VERIFICATION OF MODEL PERFORMANCE

The verification of the new interfacial shear model was accomplished in three different ways. The results of test cases were used to compare the relative velocity calculated by the two fluid model with the relative velocity calculated using the drift flux correlation. The counter current flow limit was verified by comparing the results of test cases with the data correlation using the Kutaladze numbers. Finally, the model results were compared with data from the pressure suppression test facility.

The two fluid model uses the interfacial shear to attain equilibrium between phases velocities. The relative velocity calculated using the interfacial shear should be the same as the relative velocity calculated using the drift flux correlation. The two fluid velocity could be slightly less, however, if the test case did not allow a sufficient distance for the relative velocity to relax to the equilibrium value. Figure 4 shows the comparison between the two fluid and the drift flux relative velocities.

CCFL was verified by comparing the results of test cases with hand calculations of the correlation. Figure 5 shows typical results of these comparisons using arbitrary values of K and m (similar results were obtained for several values of the empirical parameters in Equation (3.24)).

The comparison of the calculated void fractions for a PSTF blowdown with test data is shown in Figure 6. The mass balance error that is prevalent in TRAC vessel calculations causes the calculated void fraction to be above the test data. The mass balance error for the test case in Figure 6 was 8.5 per cent. In Figure 7 is shown a comparison of the pressure and in Figure 8 a comparison of the mass flow at the break for the same PSTF blowdown experiment.

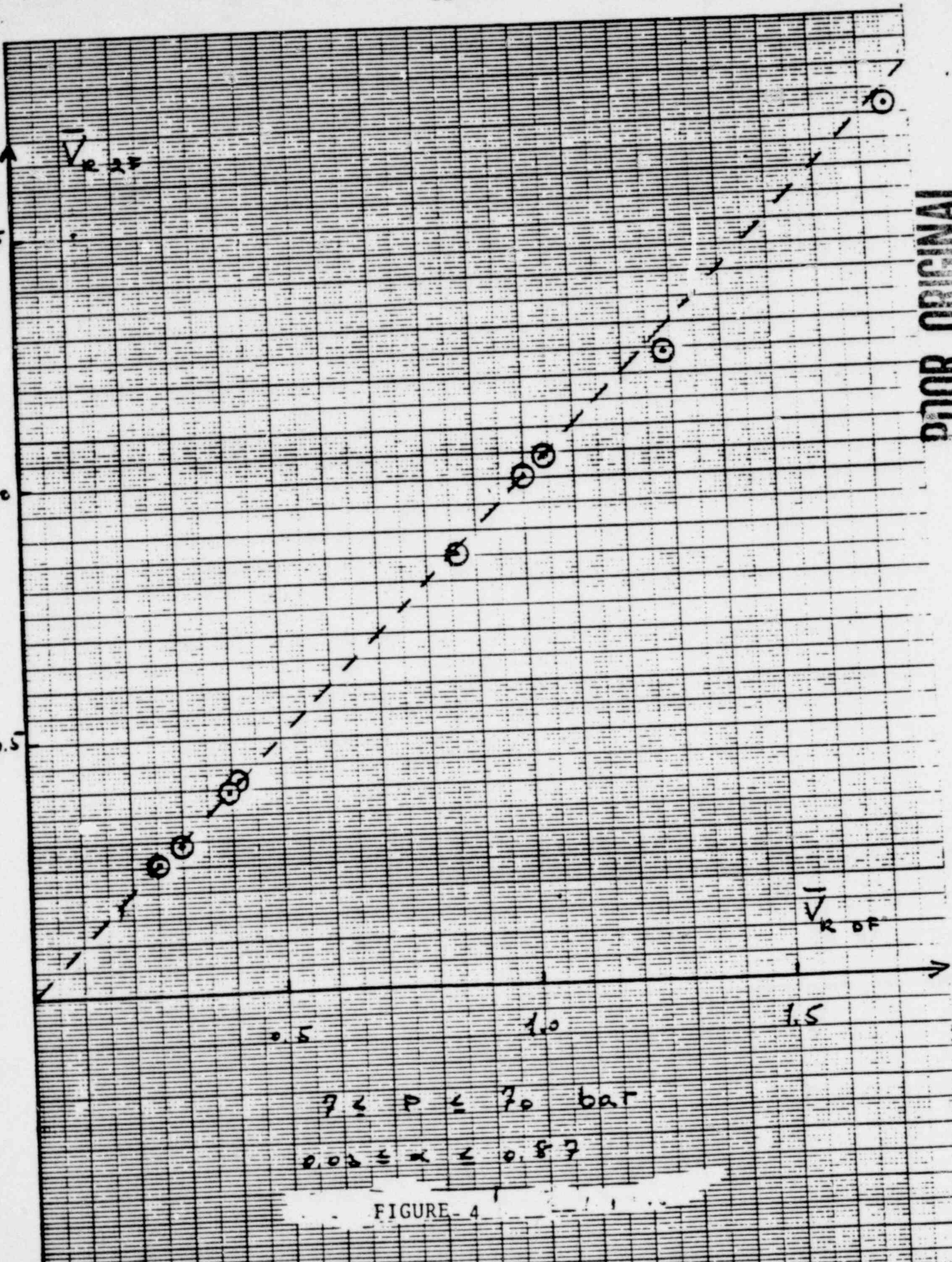

FIGURE 4

POOR ORIGINAL

CCFL COMPARISON

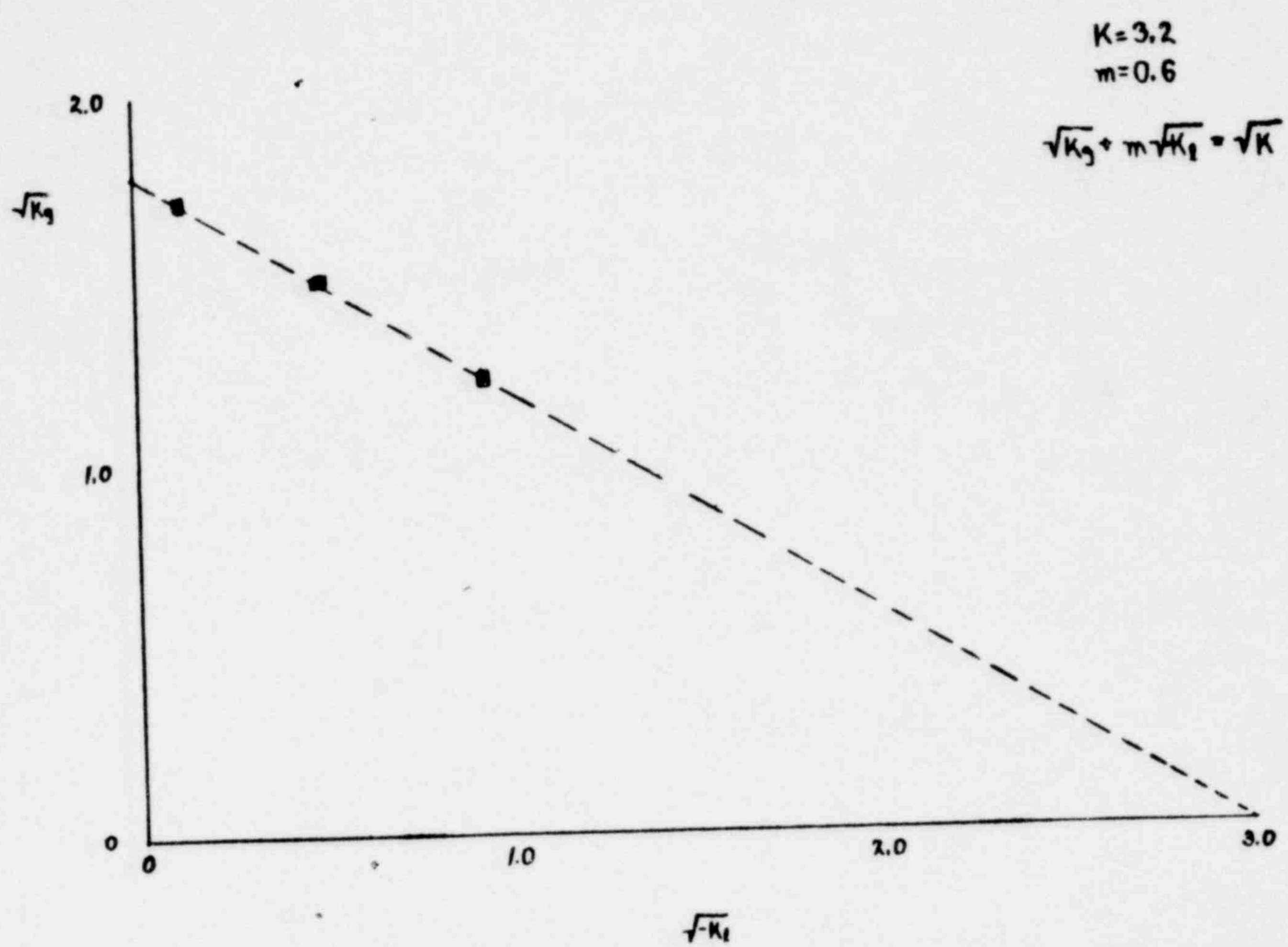

FIGURE 5

1402 306

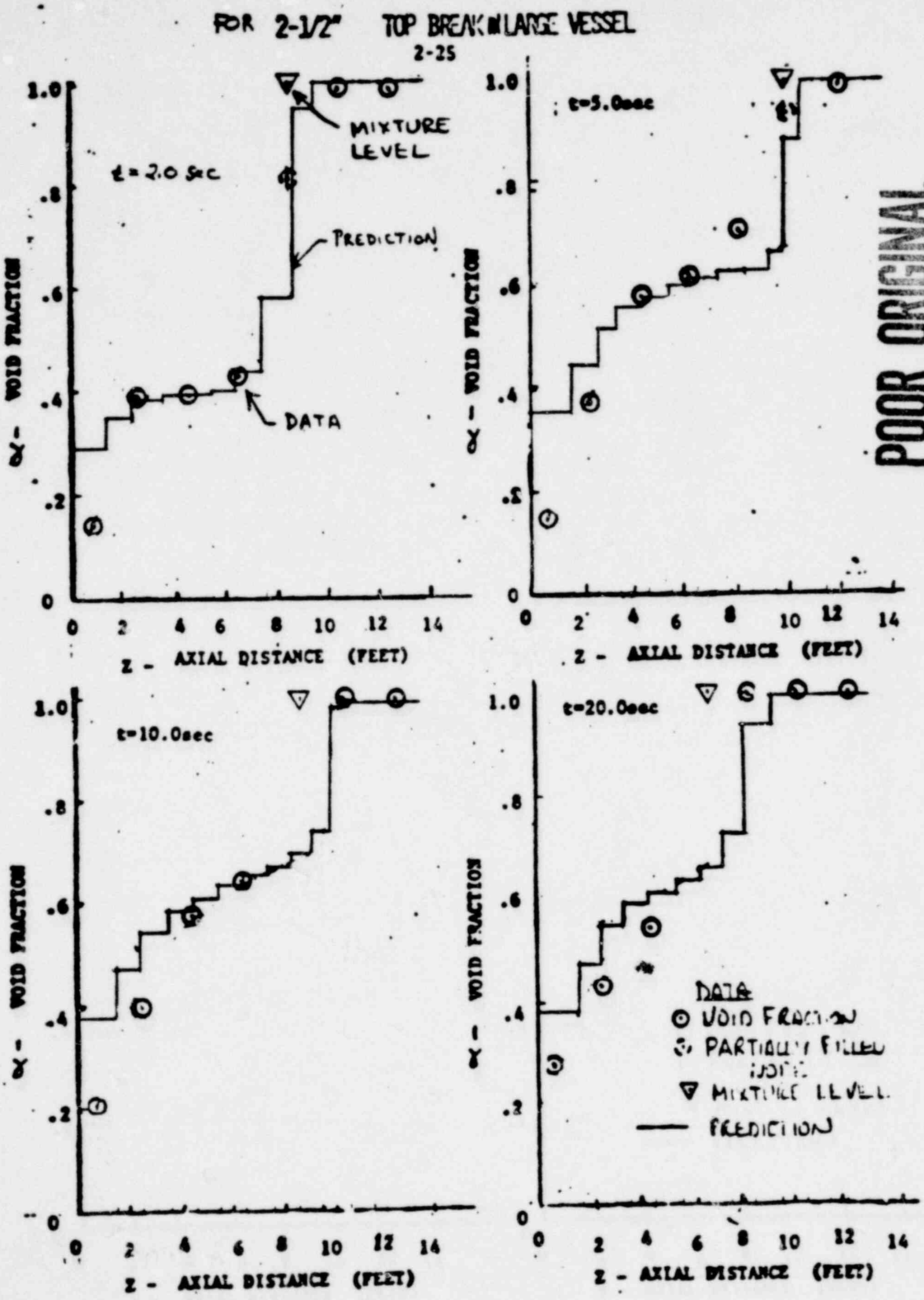

POOR ORIGINAL

LEVEL COMPARISON

FIGURE 6

1402 307

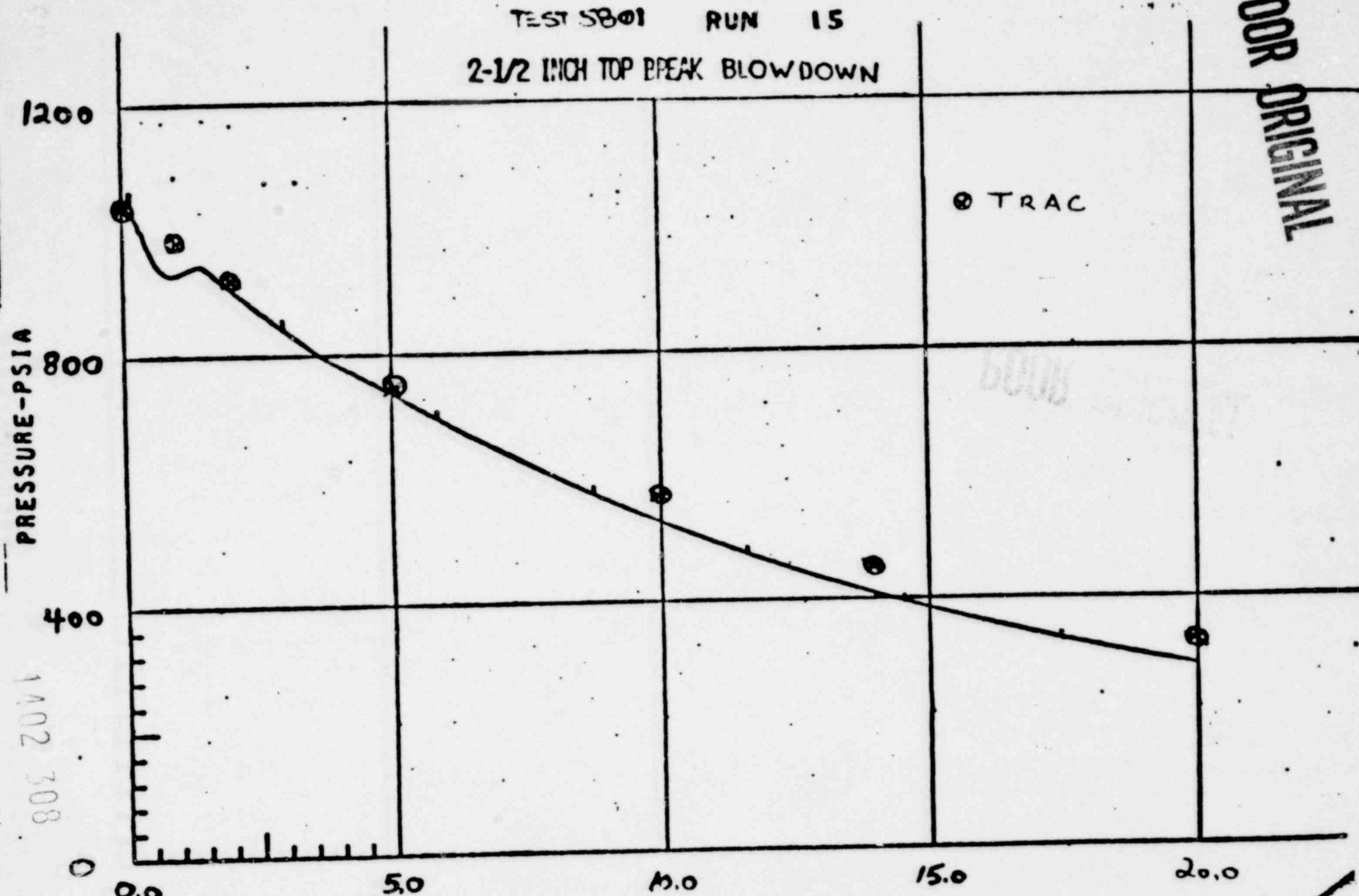

FIGURE 7 System Pressure Comparison

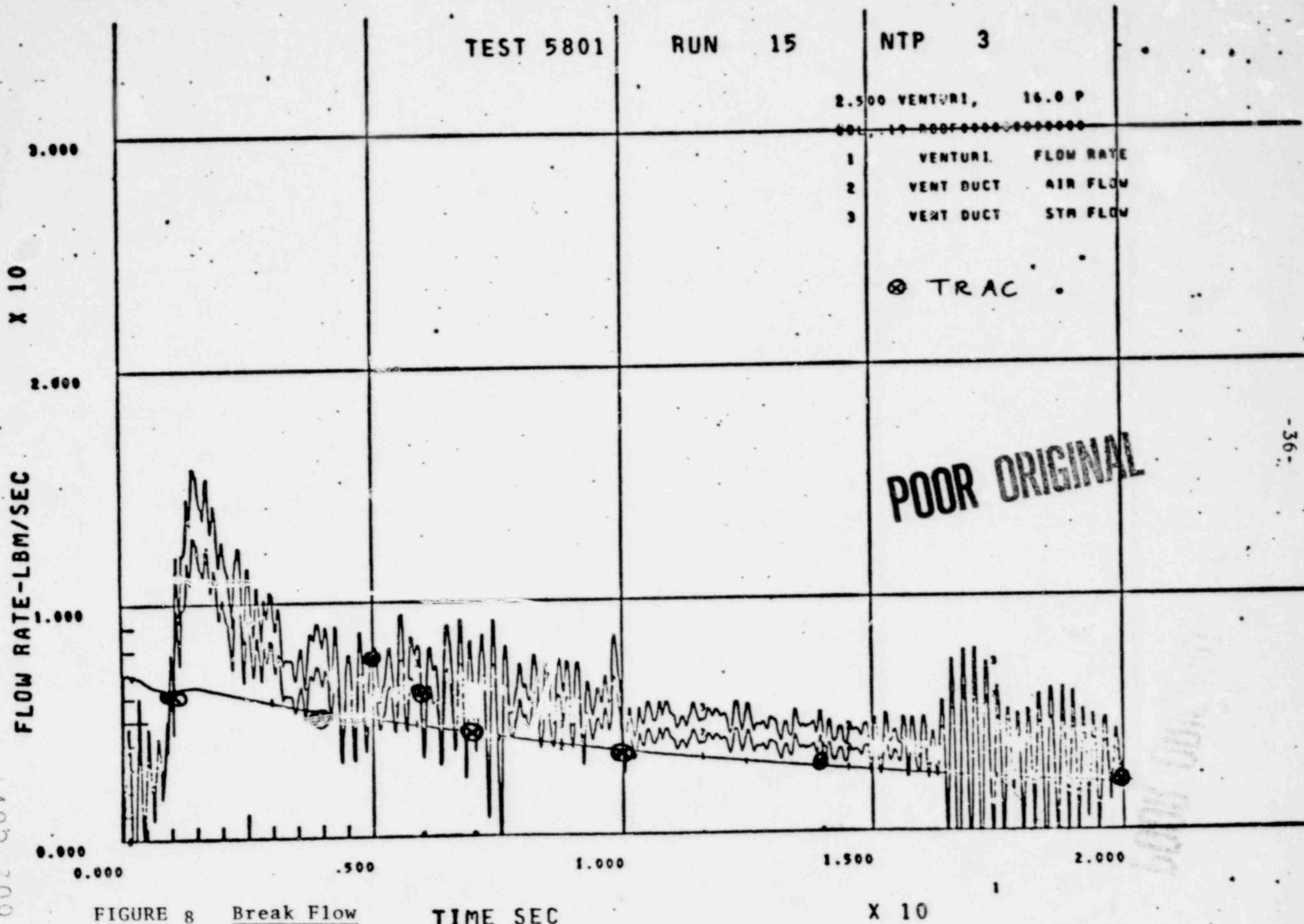

FIGURE 8 Break Flow Comparison

6. DISCUSSION AND CONCLUSIONS

A model for the partitioning of the wall friction between the phases and for the interface srag has been developed. Based on the assumption of uniform phase distribution the interface drag has been correlated from existing void-fraction correlations, and good results have been obtained.

However, the model is still preliminary and further work is necessary to finish the model. In a more rigorous model, the phase-distribution would be correlated directly and the interface drag would be correlated in terms of a drag coefficient and the interface area. Furthermore, the virtual mass would include the effect of spatial accelerations.

7. REFERENCES

1. TRAC-P1A, An Advanced Best-Estimate Computer Program for PWR LOCA Analysis, LASL, 1979.
2. M. Ishii, One-Dimensional Drift-Flux Model and Constitutive Equations for Relative Motion Between Phases in Various Two Phase Flow Regimes, ANL-77-47, October, 1977.
3. N. Zuber and J. A. Findlay, Average Volumetric Concentration in Two-Phase Flow Systems, ASME, J. Heat Transfer, November, 1965.
4. J. H. Kim, Interfacial Shear Model for TRAC Code, Letter, June 8, 1979.
5. J. H. Mahaffy, A Stability Enhancing Two Step Method for One Dimensional Two-Phase Flow, NUREG/CR-0971, LA-7951-MS, August, 1979.

8. ACKNOWLEDGEMENT

The authors gratefully acknowledge the many helpful suggestions from Drs. B. S. Shiralkar, J. H. Kim, and M. M. Aburomia, who also created the test deck for the PSTF comparison.